A Peer Reviewed International Journal of Asian Academic Research Associates

AARJMD
ASIAN ACADEMIC RESEARCH JOURNAL OF MULTIDISCIPLINARY

BEHAVIOR OF GEOGRIDS UNDER STRIP FOOTING RESTING ON SANDY SOIL

TAWFEK SHEER ALI[1]; RAID R. AL-OMARY[2]; ZEYAD S. M. KHALED[3]

[1]Assistant Lecturer, Department of Civil Engineering, College of Engineering, Kufa University, Najaf, Iraq, PhD researcher in Alnahrain University, Baghdad, Iraq,
[2]Professor of Geotechnical Engineering, Department of Civil Engineering, College of Engineering, Alnahrain University, Baghdad, Iraq,
[3]Assistant Professor of Construction Management, Department of Civil Engineering, College of Engineering, Alnahrain University, Baghdad, Iraq,

Abstract

A study of the behavior of two types of geogrids used to reinforce sandy soil under strip footings. Three layers of Netlon CE121 and Tensar SS2 geogrid were used. A series of a laboratory tests were performed to compare the estimate a bearing capacity of sand with and without using geogrids. The aim of the study is to measure the strain and elongation occurring in the ribs of Tensar SS2 geogrid only. TML strain gauges and other required accessories are used for this purpose. The soil is loaded with a rate of loadings 1 mm/s in order to simulate a static loading case with relative density of sand as 71.8 % using raining technique. It is found that the use of geogrids gives a bearing capacity with geogrid to bearing capacity without geogrid (BCR) of 1.9 and 2.5 for Netlon CE121 and Tensar SS2 respectively. The results founded also that the strain and elongation decrease gradually when the depth under footing increases as well as the distance from the centerline of footing. The strain in geogrid ribs approaches zero at a depth of about the width of footing (B) and a distance of about 3.6B from the centerline of footing. The strain and elongation have vanished in the third layer located at depth B beneath the footing.

Keywords : sandy soil, bearing capacity, Tensar SS2 geogrid, Netlon CE121 geogrid, strain and elongation of geogrid.

1. INTRODUCTION

The term *reinforced soil* describes any soil mass which has had its shear strength improved by combining it with resisting elements; these resisting elements, or reinforcement may take the form of bars, strips, tubes, grid or sheets. Reinforcement can be used as either a permanent component of a reinforced soil structure or simply to provide a temporary increase in soil shear strength to allow the construction of an adjacent structure. The observed increase in soil shear strength of a reinforced soil is always a direct result of relative soil-reinforcement displacement (Pedley, 1990).

Fannin (1986) studied the mechanisms by which a geogrid acts to reinforce a granular layer over soft clay with reference to trafficking of unpaved roads. Both model and full scale physical tests are performed. Model tests were carried out for monotonic and cyclic loading of a dual footing on a layer of granular material that was compacted over a consolidated kaolin sample. The tests were made in conditions of plane strain at a quarter scale, and included a scaled geogrid at the base of the granular layer. Measurements of footing load, displacements and photographic observations through a Perspex front face to the test box were used to identify the reinforcing actions of the geogrid. The results for both reinforced and unreinforced layers analyzed by a virtual work procedure. Load tests were made on footing plates at full scale, involving a similar of compacted granular layers over prepared London clay and including a high strength polymer geogrid. a qualitative assessment of the model performance and the reinforcing mechanisms attributed to the geogrid was resulted from the examination.

Al-Omari et al. (1987) used a steel discs and the plastic geomesh Netlon CE121 as reinforcing materials to investigate the relation of interlocking mechanism to the aperture size (T) of the geogrid mesh. Triaxial compression tests on 100 mm diameter sand samples was conducted. Perforations performed with constant diameter systemically into each steel disc. The ratio of the aperture size of the steel mesh to the grain size of the sand D_{50} was varied in the test but the area of holes to the area of solid is kept constant in each disc. The conclusions of the study is summarized throughout the following points as the strength enhancement in mesh reinforced sand depends on the mechanism of interlocking which is in turn affected by the ratio of aperture size to particle diameter. The peak stress ratio ($\sigma 1/\sigma 3$) of mesh reinforced

sand increases to a maximum at $T/D_{50} \approx 13.5$ and then drops beyond this value. The use of plastic mesh with the appropriate stiffness and the appropriate aperture size makes the strength of the sand approximately independent of the sand density.

Hameed (1990) used dried sand (ARAR) passing through sieve No.4 and five types of geogrid polymer reinforcement were used: Netlon CE111, Netlon CE121, Tensar SS1, Tensar SS2 and Tensar SS3 in two main series, pull-out tests and impact-load tests, using five types of reinforcement at different depths of the top most reinforced layer (u) and different number of layers (N). It has been concluded that the pull-out resistance increased with increasing the depth of the top most reinforcement layer, the number of the reinforcement layers and the stiffness of the reinforcement. The resistance of soil due to impact load improved with the use of reinforcement. It was observed that the peak value occurs at u=B/3 (where B is the width of footing). No significant improvement in the efficiency for the layers of reinforcement more than three.

Patra et al. (1998) presented laboratory model test results for the ultimate bearing capacity of a strip foundation supported by multi-layered geogrid-reinforced sand. The depth of embedment of the model foundation, d_f, was varied from zero to B (width of foundation). Only one type of geogrid and one type of sand at the same relative density were used. The ultimate bearing capacities obtained from the tests have been compared with the theory developed by Huang and Menq (1997). They concluded that for the same soil, geogrid and its configuration, the ultimate bearing capacity and BCR increases with the increase in embedment ratio df/B and The theoretical relationship for ultimate bearing capacity developed by Huang and Menq (1997) provides somewhat conservative predictions.

Shin and Das (2000) conducted small-scale laboratory model test results the ultimate bearing capacity of a strip foundation supported by sand reinforced with multiple layers of geogrid. Only one type of sand and one type of geogrid were used. Tests were conducted for surface foundation conditions and for foundations at various depths; the foundation depths were limited to less than the width of the foundation. Based on the test results, for a given thickness of the reinforcement zone, the bearing capacity ratio increases when the depth of the foundation is greater than zero.

Lovisa et al. (2010) investigated experimentally the degree of improvement generated by prestressing the geosynthetic layer for several embedment depths of a footing resting on a reinforced sand bed. Laboratory physical model tests and finite element analyses were conducted to study the behavior of prestressed geotextile-reinforced sand bed supporting a loaded circular footing. The addition of prestress to the geotextile reinforcement results in significant improvement to the settlement response and the load-bearing capacity of the foundation. For a surface footing, the load-carrying capacity at 5 mm settlement for the prestressed case (with prestress equal to 2% of the allowable tensile strength of the geotextile) is approximately double that of the geotextile reinforced sand without prestress. The beneficial effects of the prestressed geotextile configuration were evident for greater footing depths, in comparison with unreinforced and reinforced (without prestress) counterparts. Experimental and numerical results were also used to validate a few empirical relationships, which are commonly used for solving soil-structure interaction problems. The results obtained from finite element analysis using the program, PLAXIS are generally in reasonable agreement with experimental results.

2. MATERIALS AND TESTING

2.1 Materials

The soil used is SP sand with a the chemical and physical properties shown in table 1. sieve analysis carried out its grain size distribution according to ASTM (D422-2007) is shown in Fig. 1. The soil was classified as ***SP*** type (***Poorly graded sand, gravelly sand, little or no fines***) according to the Unified Soil Classification. ASTM (D4253-2007) and ASTM (D4254-2007) were used to determine the maximum and minimum dry unit weight. The principle for achieving a relative density larger than 70% was used to fill the box of test. To achieve that, the raining technique using a special equipment as shown in Fig. 2 is adopted. The porosity was measured by placing 6 cylindrical density pots under the moving hopper to collect the sand. The inside dimensions of the pots are 80 mm in height and 80 mm in diameter, a pot diameter larger than 3 inches was chosen to satisfy the requirements specified by Kolbuszewski (1948) for free fall method. deposition of sand, the pots were carefully collected and the excess sand leveled off using a straight-edge. The pots were then individually weighed. With the known value of the specific gravity, the porosity can

be calculated. The calibration was performed twice for the second and third layer of sand deposit before starting the test. A height of drop of (800 mm) was chosen which gave a placing density of 16.7 kN/m^3, which corresponds to a working void ratio, porosity and relative density of (e =53.9%), (n = 35%) and (RD = 71.8%) respectively. Netlon CE121 and Tensar SS2 geogrids are used. The typical properties of these types are shown in tables 2 and 3 respectively. TML strain gauges, ***SB*** tape and compatible adhesive type ***CN*** shown in Fig. 3 are used to measure the strain occurring in the ribs of geogrid.

Table 1. Chemical and physical properties of the soil

The chemical Properties	
So_3	0.53%
T.D.S	0.73%
Gypsum	1.15%
The physical properties	
G_s	2.62
Υ_{dmin} e_{max}	13.8 kN/m^3
Υ_{dmax} e_{min}	18.2 kN/m^3
Υ_{dused}	16.7 kN/m^3
e_{used}	53.9%
n_{used}	35%
$Ø_{used}$	40°
$R_{D\ used}$	71.8%
O.M.C	9.8%
D_{60} D_{50}	0.65mm 0.52mm
C_u	3.6
C_c	0.93
m.c	5.3%

Table 2. Typical properties of Netlon CE121 geogrid

Property	Units	Data
Polymer	-------	PP
Mesh type	-------	Diamo
Color	-------	Black
Packing	-------	Rolls
Unit weight	kg/m^2	0.74
Dimensions		
Aperture size	mm	6 × 8
Rib thickness	mm	1.6/1.4
Rib width	mm	2/2.75
Junction	mm	2.75
Roll width	m	4
Roll length	m	50
The mechanical properties		
Peak Tensile Strength	kN/m	6.4
Elastic modules	Gpa	0.39
Upper yield strength	Mpa	5
Lower yield strength	Mpa	5
Tensile strength	Mpa	9
Non-proportional extension strength	Mpa	6
Total extension strength	Mpa	5
Fracture elongation	%	-99
Elongation at maximum load	%	6
Total elongation	%	11

Table 3. Typical properties of Tensar SS2 geogrid

Property	Units	Data
Polymer	-------	PP
Minimum carbon Black	%	2
Roll width	m	4
Roll length	m	50
Unit weight	kg/m^2	0.29
Roll weight	kg	60
Dimensions		
A_L	mm	28
A_T	mm	40
W_{LR}	mm	3
W_{TR}	mm	3
t_J	mm	3.8
t_{LR}	mm	1.2
t_{TR}	mm	0.9
Rip shape	Rectangular with square edges	
The mechanical properties		
Peak Tensile	kN/m	14.4/2
Elastic modules	GPa	0.57/0
Upper yield	Mpa	1 /3
Lower yield	Mpa	1/3
Tensile strength	Mpa	24/30.
Fracture	%	-98/-
Percentage	%	3.5/2.
Total percentage	%	5/4.25

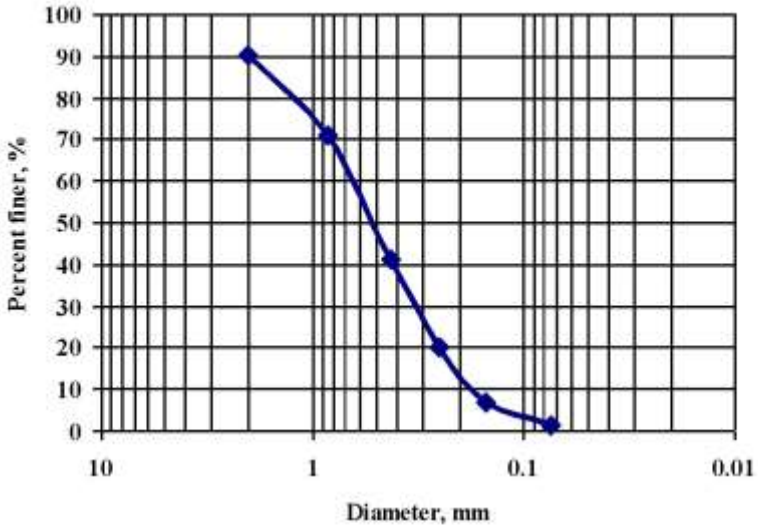

Figure 1. Grain size distribution of soil

Figure 2. Raining technique equipment

Figure 3. TML strain gauges, ***SB*** tape, and compatible adhesive type ***CN***

The weight of every empty pot was measured using a sensitive balance and the volume of pots was accurately determined by measuring the weight required to fill each pot. After the air dried sandy soil was placed in the box according to the raining technique, i.e. maintaining a dropping height of 800 mm in three layers, the thickness of each layers is 200 mm. After each test, the sand box should be completely emptied.

A Triaxial test is performed to estimate the angle of internal friction and cohesion of soil. The angle of internal friction Ø° is found to be 40° at peak strain level and the cohesion is zero. The model box have a dimensions 1 m length, 0.5 m width and 0.6 m depth. A steel plate with 0.48 m length, 0.135 m width and 0.01 m thickness used to represent a footing model. The loading frame and the required accessories are shown in Fig. 4.

2.2 Model Configuration

The model is performed as shown in Fig. 5. The strip footing model is placed on the top of the soil surface in the model test box. The first layer of geogrids is placed at a depth of (u) equals to 0.25B. The leftover depth is divided into two intervals, each of 0.375B. The same procedure is performed for the two types of geogrids. The tests conducted under plane strain conditions included the employment of side wall

lubrication and wide tank with a loading frame. The tank dimensions are 500 mm × 600 mm × 1000 mm in width, height and length respectively, the strip footing dimensions are 135 mm × 480 mm in width and length respectively.

Figure 4. Loading frame and required accessories

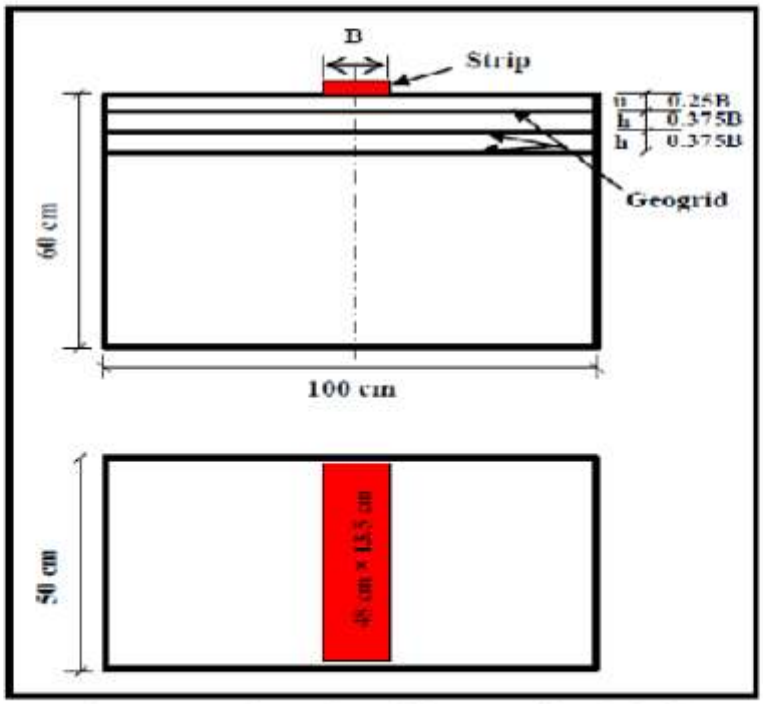

Figure 5. Geometry and top plan of the geogrid and footing model

2.3 The Datatronic 128-channel Automatic Data Acquisition System

The 128-channel automatic data acquisition system has been designed and created to satisfy the requirements of all laboratories, even the most complex ones, and to considerably improve laboratory productivity and cost effectiveness. Data collection takes place completely automatically. A Windows based program with menu driven command selection is straightforward and easy to follow and does not require the attention of a skilled operator. The device is capable of acquiring inputs from any type of transducer: Strain Gauge Bridge, LVDT (Linear Variable Differential Transformer) with optional adapter, Potentiometer. A continual live display of test diagrams is provided in addition to test data exportation with TXT files for consecutive processes, with Excel or other SW. A personalized printout of certificates and test diagrams is available. System configuration facilitated by a 5 key membrane keyboard with encoder for rapid setting. The system allows memorization of every configuration and calibration. Data logging (from the PC using the Windows based program) is facilitated by user-friendly software included in the Datatronic package. The system allows setting for each channel the sampling type in linear form, square root form, logarithmic form and personalizable form, with frequencies from very fast (one second) to infinite, without reading limits (storage limits are linked to PC memory), with the possibility of delaying the start time.

The dimensions of the unit are: 460 × 540 × 350 mm and Weight: 12 kg as shown in Fig. 6.

Figure 6. The datatronic 128-channel automatic data acquisition

2.4 Calibration Method

The datatronic 128-channel automatic data acquisition system reads the strain through an electric circuit as divisions. The readings were calibrated using using single rib of geogrid and the strain gauge was fixed on the middle of the rib and tested by the computer controlled electronic universal testing machine. The strain gauge connected to strain gauge amplifier which by turn connected to the datatronic 128-channel automatic data acquisition system. The computer controlled electronic universal testing machine records the strain against time, the datatronic acquisition system records the divisions against the same time. Accordingly a calibration between divisions and strains was carried out and the following equation was obtained with coefficient of determination $r^2 = 0.9689$

$$\epsilon = 5R\ 10^{-8} + 0.0002$$

Where

R: is the reading of the automatic data acquisition system (divisions).

The output reading of the unit is a strain (ε), the elongation (Δl) can be given by multiplying the strain (ε) by the rib length (l).

3. TESTS RESULTS

3.1 Un-reinforced soil model test results

The model is performed to the test of footing on soil without geogrid. The ultimate bearing capacity and load-settlement relation is shown in Fig. 7. The rate of loadings is 1 mm/s as a static loading. The footing was placed on the upper free surface of soil. The values of bearing capacity considered as a base value to investigate the improvement of soil using the geogrid. From The relationship between bearing capacity and relative settlement (s/B %) of soil, it can be seen that the ultimate bearing capacity obtained for the strip footing was 234.3 kPa. The relative settlement at the ultimate bearing capacity is 11.1%. The point of ultimate bearing capacity was easily marked on the load-settlement curve since the test is strain-controlled and the peak is clearly visualized.

3.2 Reinforced soil model test results

Tests are performed to study the effect of using geogrids to improve the bearing capacity of soil. Two types of geogrids (**Netlon CE121 and Tensar SS2**) are used. The relation between the ultimate bearing capacity (q) and the relative settlement (s/B %) is plotted as shown in Fig. 8. From the figure it can be seen that **Tensar SS2** type give a higher improvement in bearing capacity than the **Netlon CE121**. The bearing capacity ratio (BCR) is the ratio of bearing capacity with geogrids to the bearing capacity without geogrid. For **Netlon CE121** geogrid, the (BCR) is **1.9** and for **Tensar SS2** is **2.5**. This is because of **Tensar SS2** strength is higher than **Netlon CE121**. The results give indication to which type of geogrids may provide better improvement of soil bearing capacity.

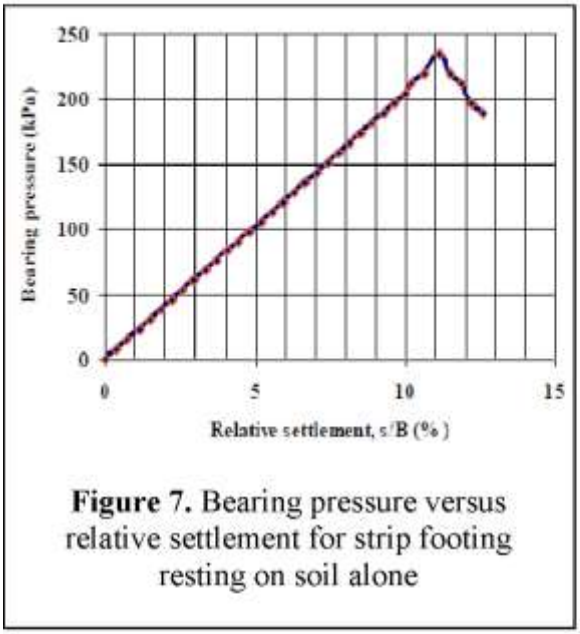

Figure 7. Bearing pressure versus relative settlement for strip footing resting on soil alone

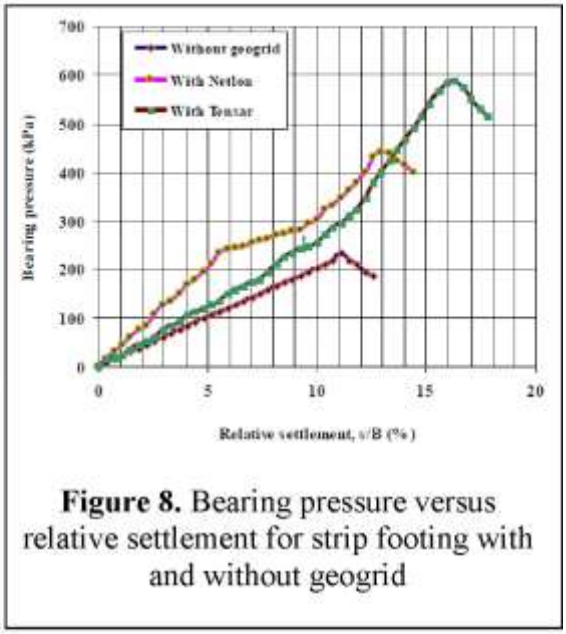

Figure 8. Bearing pressure versus relative settlement for strip footing with and without geogrid

3.3 Strain and Elongation Measurement Results

On scrutiny of the nationally and internationally available literature, it appears that there is previous work on the straining mechanism occurring in the geogrid ribs during the application of foundation loading where the failure is progressive. The distribution of strains in the geogrid ribs is very important to understand the enhancement mechanism of bearing capacity, to what extent there is a need to high stiffness/strength geogrids, and at which stress level the soil-grid bond may break. To begin the tests with strain gauges for the strip footing, the strain gauges be distributed

to cover one side of footing reinforcement because of similarity of both sides. Strain gauges are fixed on the long rib because it has a higher strength and modulus of elasticity than the short rib. The transverse direction (XMD long rib) of Tensar SS2 was placed in the sand container in the direction of lateral strain (long direction of sand container) during loading in order to gain higher improvement. Fixing of strain gauges on the mesh of geogrid and the distribution of strain gauges are shown in Fig. 9. Table 4 shows horizontal distances of the strain gauges from the centerline of strip footing. The same distribution is repeated for the second and third layer. The centerline of the mesh of geogrid coincides with the centerline of strip footing. The arrangement of strain gauges is chosen with equal distance from the centreline of footing to the edge of mesh.

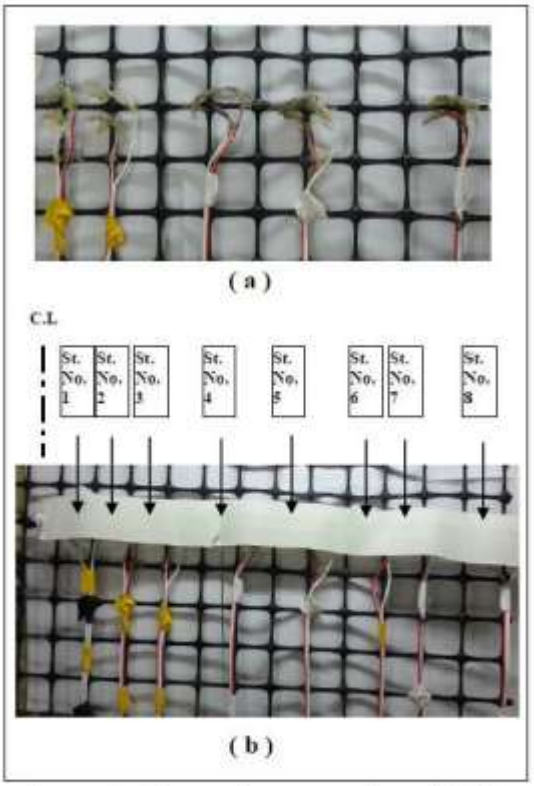

Figure 9. (a) pasting operation. (b) The distribution of strain gauges

Table 4. Horizontal distances of the strain gauges from the centerline of strip

Strain gauge number	Distance of gauge (S) from the centre of footing (mm)	Relative distance (d/B) of gauge from centre of footing
1	40	0.295
2	80	0.593
3	120	0.889
4	200	1.48
5	280	2.074
6	400	2.96
7	440	3.259
8	480	3.6

3.4 Horizontal and vertical strain distribution results

The distribution of strains occurring in strain gauges which are fixed on the geogrid ribs are demonstrated in Figs. 10 and 11. The values shown are recorded at the ultimate bearing capacity. Table 4 had already show the distances of strain gauges shown in Fig. 10. The distance of the geogrid layers represent the distance of strain gauges under the footing in Fig. 11.

Figure 10 demonstrates the relationship between the horizontal distance, relative distance, and strain. It has be found that the values of strain decrease when the strain gauge distance from the centerline of footing for each layer increase. The location of the farthest strain gauge the value of 3.6B, which indicate the zone of the effect of stress.

Figure 11 shows the relationship between the horizontal distance, relative distance, and elongation in geogrid ribs. They have the same behavior as in Fig. 10 because of the linear relationship between the strain and elongation.

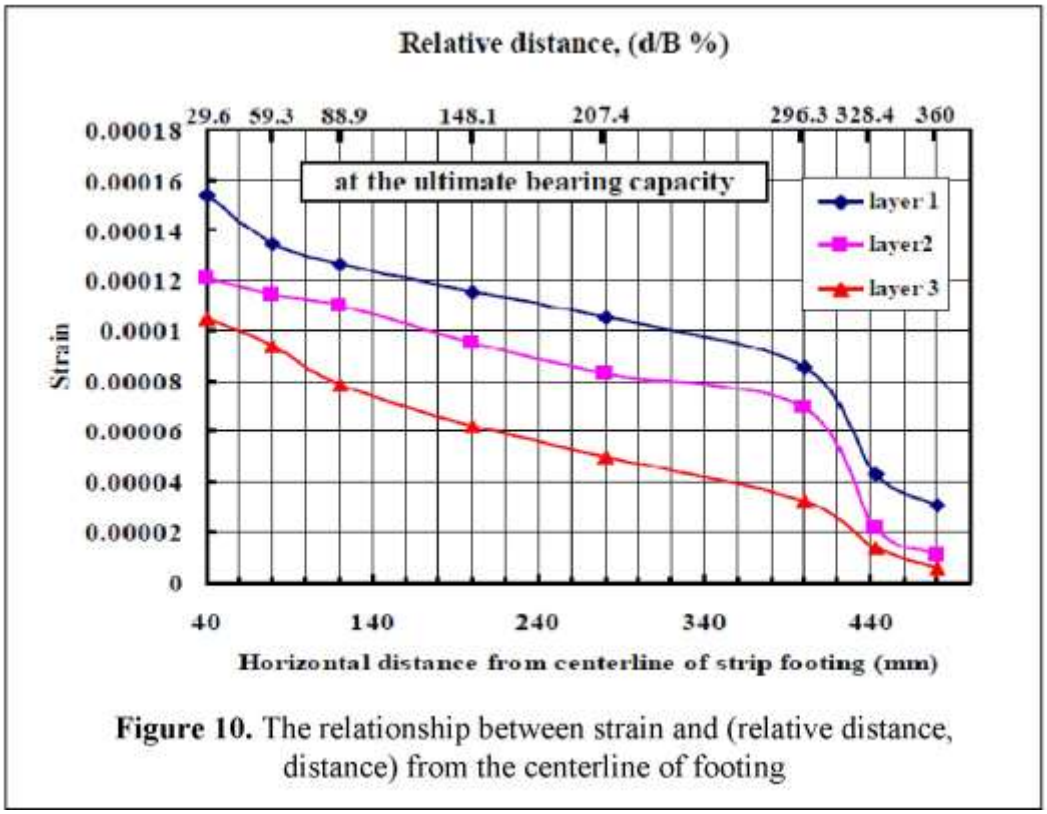

Figure 10. The relationship between strain and (relative distance, distance) from the centerline of footing

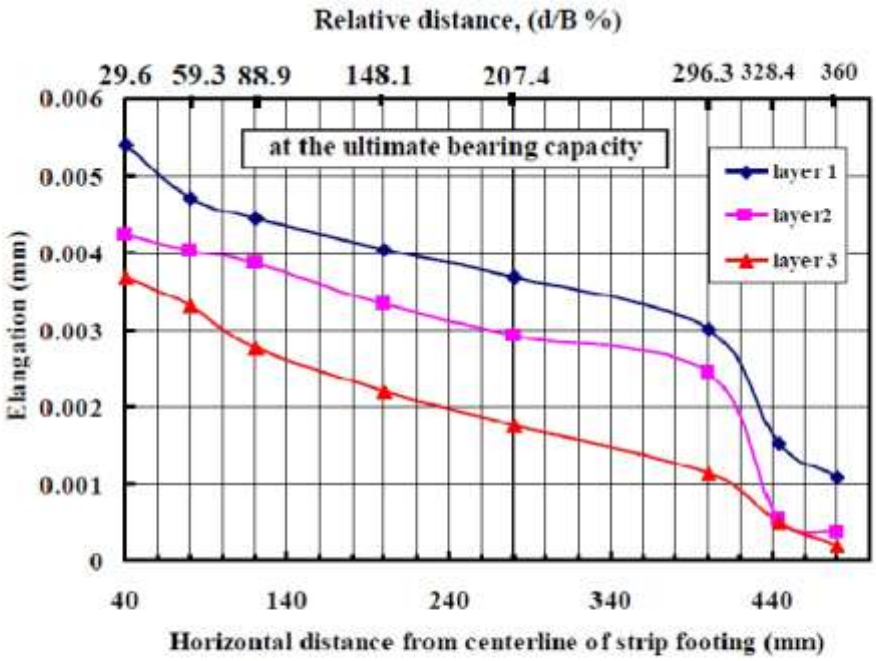

Figure 11. The relationship between elongation and (relative distance, distance) from the centerline of footing

Figure 12 shows the relationship between the depth of strain gauges which are represented by the depth of geogrid mesh under the footing and depth, relative depth. The relationship is drawn for the values of strain at the ultimate bearing capacity. Strain decrease as the depth under footing increase slightly. The values of strain decrease to a small value for the third layer and for the furthest strain gauge.

Figure 13 explains the relationship between elongation and depth, relative depth of strain gauges. The relationship shows how the values of elongation in each rib of geogrid mesh. The elongation decrease as well as the depth increases. The elongation of strain gauges in the furthest layer and location are very small, that decided the results of researcher which are represent that the three layer of geogrid and 3.6B is the zone of soil stress in reinforcement soil by geogrid.

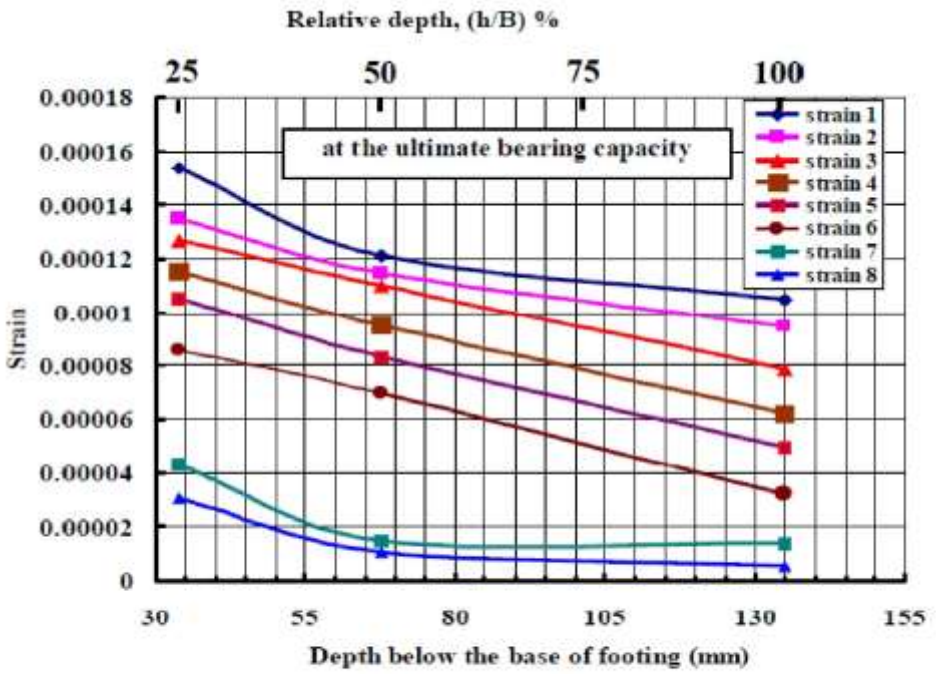

Figure 18. The relationship between strain and (relative depth, depth) below the base

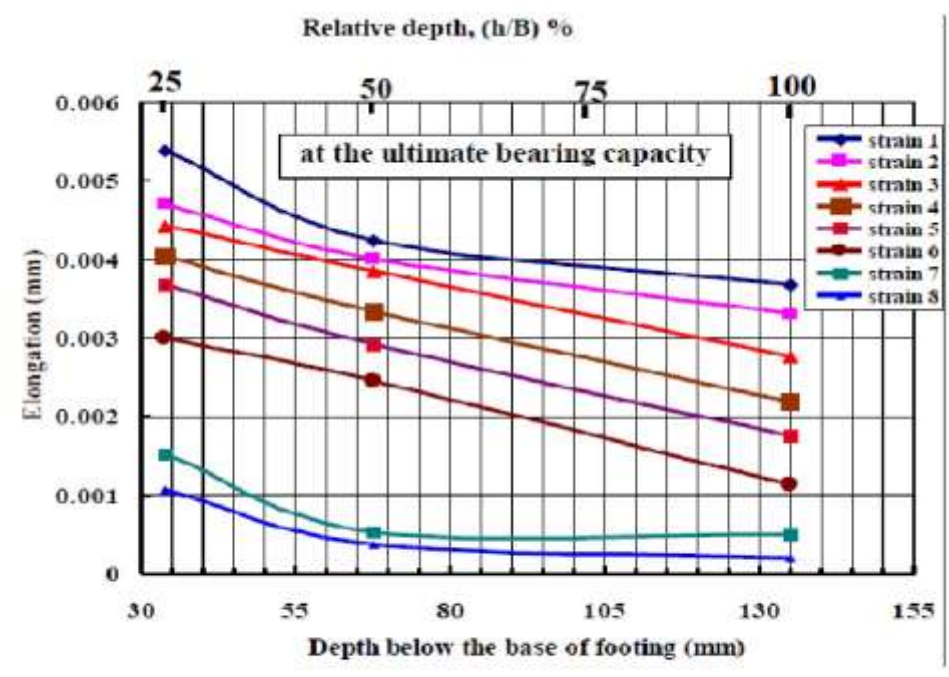

Figure 19. The relationship between strain and (relative depth, depth) below the base

4. CONCLUSIONS

The main experimental program involved bearing capacity tests using strip footing model resting on sand with and without reinforcement. A special experimental program was designed to investigate the behaviour of strain occurring in the ribs of geogrid during the bearing capacity tests using the appropriate strain gauges, a problem which is not covered yet. Based on the experimental and numerical study the following conclusions may be drawn:

1- The highest values of obtained BCR are 1.9 when using Tensar SS2 and 2.5 when using Netlon CE121.
2- The relative settlement at failure increases with the increase in the bearing improvement ratio (BCR).
3- A significant effect on enhancing the ultimate bearing capacity of strip is the geogrid rib stiffness; it appears that BCR increased when the stiffness becomes higher
4- The effect of the horizontal distance from center line of footing and the vertical depth underneath footing base is very significant on the strains and elongations occurring in the geogrid ribs.
5- The strain and elongation of rib decrease along the horizontal direction away from center of footing and also decrease in the downward direction underneath footing base.
6- The strain and elongation have vanished in the third layer located at depth B beneath the footing.

REFERENCES

Al-Omari, R. R., Al-Dobaissi, H. H. and Al-wadood, B. A., (1987), "Inextensible Geomesh Included in Sand and Clay", Prediction and Performance in Geotechnical Engineering/Calgary/17-19 June, pp. 155-160.

ASTM D1388-96, (2007), "Standard Test Method for Stiffness of Fabrics".

ASTM D1505-03, (2007), "Standard Test Method for Density of Plastics by the Density-Gradient Technique".

ASTM D1777-96, (2007), "Standard Test Method for Thickness of Textile Materials".

ASTM D422-63, (2007), "Standard Test Method for Particle Size-Analysis of Soils".

ASTM D4253-2007, "Standard Test Method for Maximum Index Density and Unit Weight of Soils Using a Vibratory Table".

ASTM D4254-2007, "Standard Test Method for Minimum Index Density and Unit Weight of Soils and Calculation of Relative Density".

ASTM D6637-01-2007, "Standard Test Method for Determining Tensile Properties of Geogrids by the Single or Multi-Rib Tensile Method".

ASTM D792, (2007), "Standard Test Methods for Density and Specific Gravity (Relative Density) of Plastics by Displacement".

ASTM D854-05, (2007), "Standard Test Method for Specific Gravity of Soil Solids by Water Pycnometer".

Bowles, J. E., (1996), "Foundation Analysis and Design", 5th Edition, McGraw-Hill Book Company.

E.C. Shin and B.M. Das, (2000), "Experimental Study of bearing Capacity of a Strip Foundation on Geogrid-Reinforced Sand", Journal of Geosynthetics International 2000, VOL. 7, NO. 1, pp. 59-71.

Fannin, R. J., (1986), "Geogrid Reinforced of Granular Layers on Soft Clays A Study at Model and Full Scale", Ph.D. Thesis, University of Oxford, UK.

Hameed, H. H., (1990), "Footing on Reinforced Earth Subjected to Impact Loading", M.Sc. Thesis, Baghdad University, Iraq.

Lovisa, J., Shukla, S. K. and Sivakugan, N., (2010), "Behaviour of Prestressed Geotextile-Reinforced Sand Bed Supporting A Loaded Circular Footing", Journal Geotextiles and Geomembranes, 28, pp. 23–32.

Pedley, M. J., (1990), "The Performance of Soil Reinforcement in Bending and Shear", Ph.D. Thesis, Oxford University, Britain.